Secretion of amyloidogenic gelsolin progressively compromises protein homeostasis leading to the intracellular aggregation of proteins

Lesley J. Page[a], Ji Young Suk[b,1], Lyudmila Bazhenova[b,1], Sheila M. Fleming[c], Malcolm Wood[a], Yun Jiang[d], Ling T. Guo[d], Andrew P. Mizisin[d], Robert Kisilevsky[e], G. Diane Shelton[d], William E. Balch[a,f,g,h,2], and Jeffery W. Kelly[b,h,2]

Department of [a]Cell Biology, [b]Departments of Chemistry and Molecular and Experimental Medicine, [f]Department of Chemical Physiology, and [g]Institute for Childhood and Neglected Diseases, and [h]The Skaggs Institute for Chemical Biology, The Scripps Research Institute, 10550 North Torrey Pines Road, La Jolla, CA 92037; [c]Department of Neurobiology, The David Geffen School of Medicine, University of California, Los Angeles, CA 90095; [d]Department of Pathology, University of California at San Diego, La Jolla, CA 92093; and [e]Departments of Pathology and Molecular Medicine, and Biochemistry, Queen's University, Kingston, ON, Canada K7L 3N6

Edited by Charles Weissmann, Scripps Florida, Jupiter, FL, and approved May 1, 2009 (received for review November 20, 2008)

Familial amyloidosis of Finnish type (FAF) is a systemic amyloid disease associated with the deposition of proteolytic fragments of mutant (D187N/Y) plasma gelsolin. We report a mouse model of FAF featuring a muscle-specific promoter to drive D187N gelsolin synthesis. This model recapitulates the aberrant endoproteolytic cascade and the aging-associated extracellular amyloid deposition of FAF. Amyloidogenesis is observed only in tissues synthesizing human D187N gelsolin, despite the presence of full-length D187N gelsolin and its 68-kDa cleavage product in blood—demonstrating the importance of local synthesis in FAF. Loss of muscle strength was progressive in homozygous D187N gelsolin mice. The presence of misfolding-prone D187N gelsolin appears to exacerbate the age-associated decline in cellular protein homeostasis (proteostasis), reflected by the intracellular deposition of numerous proteins, a characteristic of the most common degenerative muscle disease of aging humans, sporadic inclusion body myositis.

amyloid | proteostasis | sporadic inclusion body myositis | FAF mouse

Protein homeostasis (proteostasis) refers to the cellular control of the synthesis, structure, trafficking, and degradation of proteins (1). An aging-associated decline in proteostasis capacity may contribute to the onset of many diseases associated with protein misfolding (2–4). Inheriting an aggregation-prone protein(s) further challenges proteostasis capacity upon aging (5). Such challenges can lead to loss-of-function disorders or aggregation-associated degenerative diseases (1–3, 5–9). Whether intracellular and/or extracellular aggregation leads to proteotoxicity in diseases associated with extracellular amyloid, such as Alzheimer's disease, remains unclear (3, 10).

Familial amyloidosis of Finnish type (FAF) or gelsolin amyloidosis is thought to result from amyloidogenesis of a fragment of gelsolin causing aging-associated proteotoxicity (1, 11–14). Plasma gelsolin is a 83-kDa 6-domain Ca^{2+}-binding protein that is secreted from several cell types into the blood (>200 μg/mL) (15), with muscle contributing significantly (16). A D187 mutation to N or Y (D187N/Y) in plasma gelsolin compromises Ca^{2+} binding in domain 2 and thus folding (13). This enables aberrant cleavage by furin in the *trans*-Golgi, generating a 68-kDa fragment (C68) of gelsolin that is secreted (11, 17) (Fig. 1*A*). Only a fraction of D187N/Y plasma gelsolin in FAF is cleaved by furin; the remainder is secreted as full-length, functional plasma gelsolin. C68 can be further cleaved in the extracellular space by a type I matrix metalloprotease, like MT1-MMP (12), to generate the major (8-kDa) and minor (5-kDa) amyloidogenic fragments that deposit in blood vessel walls, skin, the autonomic nervous system, and the eye of humans, causing cranial and peripheral polyneuropathy, cutis laxa, and corneal lattice dystrophy (18). Deposition also occurs in skeletal and cardiac muscle, leading to cardiomyopathy and muscle weakness (14, 18). Given that human D187N/Y plasma gelsolin is expressed in most tissues and that the C68 fragment is in the blood, the origin of the amyloidogenic fragments (local production versus serum-derived) has been unclear, as are the events contributing to age-onset proteotoxicity.

Herein, we report transgenic human D187N gelsolin amyloidosis mouse models that recapitulate the proteolytic cascade that generates the 8- and 5-kDa gelsolin amyloidogenic peptides in FAF patients. Although C68 is found in the blood of the mice, our results indicate that circulating C68 or full-length gelsolin is unlikely to contribute to the observed amyloidogenesis. Instead, the amyloidogenic fragments are likely generated from MT1-MMP proteolysis of C68 in very close proximity to the cells making D187N C68 and are deposited locally. Furthermore, it appears that the presence of a secreted amyloidogenic protein triggers the intracellular deposition of Aβ, gelsolin, and other amyloid-prone proteins within the muscle fibers of older mice, compromising muscle function in homozygous D187N gelsolin mice. These pathological changes resemble those seen in sporadic inclusion body myositis (sIBM), suggesting that disruption of proteostasis may, in part, contribute to the etiology of sIBM (19–21).

Results

Human D187N Gelsolin Transgenic Mice Generate the FAF-Associated Fragments. Hemizygous (−/+) and homozygous (+/+) transgenic mouse models of FAF were generated by creatine kinase promoter-mediated expression of human D187N plasma gelsolin in cardiac and striated muscle (see *SI Methods*). These lines were created to express two different levels of D187N plasma gelsolin exclusively in muscle to follow the progression of gelsolin amyloidosis with age, and to assess the contributions of locally synthesized versus circulating D187N plasma gelsolin to amyloidogenesis.

Whether the murine models recapitulate the sequential proteolytic processing of D187N plasma gelsolin to afford the 8- and 5-kDa FAF-associated amyloidogenic fragments was examined. Immunoblot analysis of 18-month-old D187N (−/+) mouse tissue showed high levels of human plasma gelsolin in tissues containing cardiac or striated muscle, but undetectable, or much

Author contributions: L.J.P., W.E.B., and J.W.K. designed research; L.J.P., J.Y.S., L.B., Y.J., L.T.G., and A.P.M. performed research; L.J.P., S.M.F., M.W., Y.J., L.T.G., A.P.M., R.K., G.D.S., and W.E.B. analyzed data; L.J.P., G.D.S., W.E.B., and J.W.K. wrote the paper.

The authors declare no conflict of interest.

This article is a PNAS Direct Submission.

[1]J.Y.S. and L.B. contributed equally to this work.

[2]To whom correspondence may be addressed. E-mail: webalch@scripps.edu or jkelly@scripps.edu.

This article contains supporting information online at www.pnas.org/cgi/content/full/0811753106/DCSupplemental.

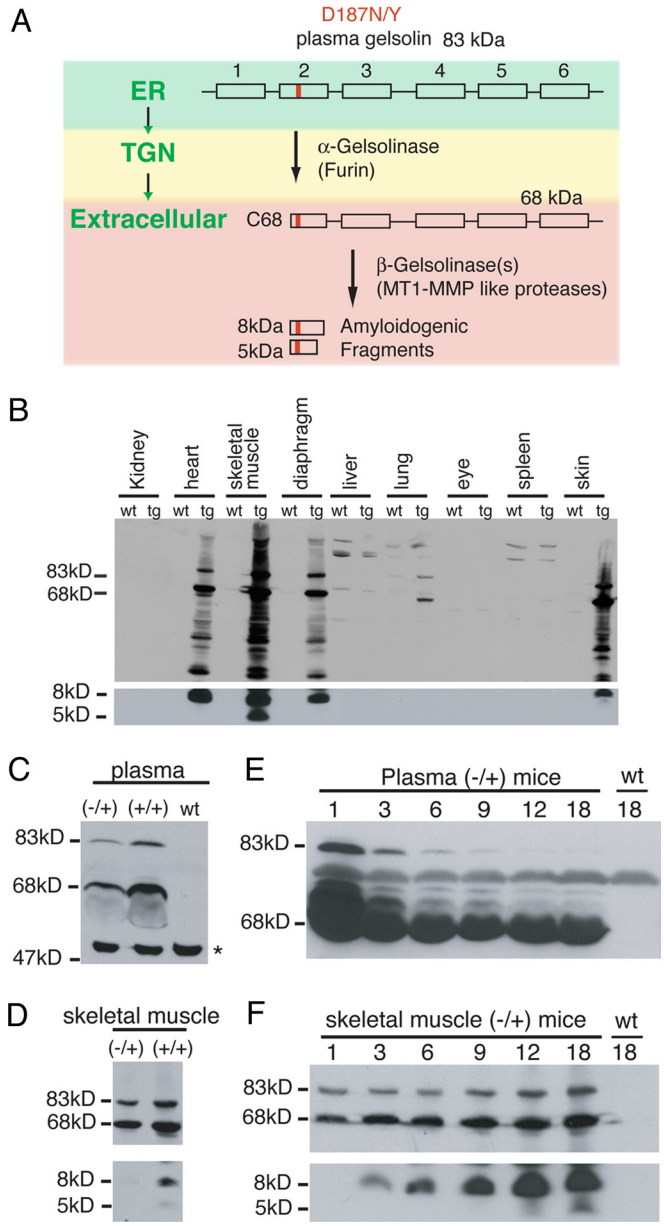

Fig. 1. Proteolytic fragments of D187N plasma gelsolin are present in transgenic mice. (*A*) Scheme of D187N/Y (mutation is highlighted in red) plasma gelsolin proteolytic cascade and cleavage products detected in FAF patients. The 6 domains of gelsolin are depicted by rectangles. The subcellular or extracellular location of each event is indicated in green. A proportion of D187N/Y is cleaved by furin in the *trans*-Golgi network (TGN) to generate a 68-kDa protein (C68) that is secreted. C68 is further processed extracellularly by MT1-MMP-like proteases, to form the 8- and 5-kDa amyloidogenic fragments that are deposited in FAF patients. (*B*) Western blot of tissues from 18-month D187N (−/+) gelsolin mice and wild-type siblings. In addition to full-length (83-kDa) plasma gelsolin, many proteolytic fragments, including the 68- and 8-kDa peptides, were detected in cardiac and striated muscle tissue from D187N (−/+) transgenic (tg) mice but not from their wild-type (wt) siblings. No or very low expression levels of D187N gelsolin were detected in nonmuscle tissues. (*C* and *D*) Homozygous D187N (+/+) mice have approximately double the level of human D187N plasma gelsolin in plasma (*C*) and skeletal muscle (*D*) compared with the hemizygous D187N (−/+) mice. The asterisk (*) indicates a cross-reacting protein that is also found in wild-type animals that do not express human D187N gelsolin. (*E*) The amount of human D187N plasma gelsolin in plasma decreases with the age of the mice (in months). (*F*) The amount of human D187N plasma gelsolin in skeletal muscle increases as the age of the mouse (in months) increases. No expression of human D187N gelsolin is detected in the wild-type animal (wt).

lower, levels in other tissues including kidney, eyes, lung, liver, and spleen (Fig. 1*B*). D187N (−/+) mice, but not their wild-type littermates, produce full-length 83- and 68-kDa (C68) human mutant gelsolin in plasma (Fig. 1*C*) and in skeletal muscle (Fig. 1*D Upper*), indicating that furin cleavage occurs.

The major 8-kDa amyloidogenic fragment expected from MT1-MMP proteolysis was present in D187N (−/+) heart, skeletal muscle (5-kDa fragment also detected), diaphragm, and skin (14, 22) (Fig. 1 *B*, *D*, and *F*), but neither amyloidogenic fragment was detected in serum, as is the case in human D187N gelsolin serum. Immunohistochemistry revealed that cutaneous muscle fibers extending into the lower dermis were likely responsible for the D187N gelsolin detected in skin.

Despite the presence of C68 in plasma, the 8-kDa fragment and its amyloid (see below) is only observed in tissues synthesizing D187N gelsolin, supporting the hypothesis that local synthesis with local MMP processing are critical for amyloidogenesis and FAF (11, 12, 23, 24). The 83- and 68-kDa D187N gelsolin plasma levels decreased as the D187N (−/+) mice age (Fig. 1*E* and Fig. S1) until they stabilized at 6 months. In contrast, the skeletal muscle levels of C68 and full-length D187N gelsolin (83 kDa) increased modestly (≈2-fold), whereas the 8-kDa fragment increased substantially (>10-fold) and the 5-kDa fragment became detectable with aging (Fig. 1*F*).

D187N (−/+) Amyloid Deposition Originates Around Endomysial Capillaries Before Appearing in the Surrounding Muscle Fibers. Electron micrographs (EM) of amyloid extracted from muscles of 18-month-old D187N (−/+) mice revealed the expected 8- to 10-nm fibril morphology and immuno-EM showed that these fibrils were composed of gelsolin (Fig. 2*A*), unlike the situation in WT littermates. Immunoblot analysis of the extracted amyloid showed the majority comprises the 8-kDa gelsolin fragment (Fig. 2*A Inset*). Full-length plasma gelsolin and C68 were notably absent from the extracted amyloid, providing evidence that their 2-fold increase in steady-state concentration in muscle with aging is probably not due to incorporation into amyloid, but more likely is due to amyloid deposition in the endomysium compromising diffusion out of muscles (site of synthesis) into the plasma.

Congo red (CR), a dye that selectively binds to amyloid, afforded its characteristic apple-green birefringence on illumination with polarized light in 18-month-old D187N (−/+) muscle, but not in WT muscle (Fig. S2) (25, 26). Cross-sections of frozen muscle specimens (vastus lateralis and cranial tibial) collected at 3, 9, and 18 months of age from D187N (−/+) mice (Fig. 2 *C–E*) and WT mice (Fig. 2*F*) were evaluated by CR fluorescence, a more sensitive amyloid indicator than CR birefringence (which was not attempted). In 3-month-old D187N (−/+) mice, amyloid CR fluorescence was limited to the vicinity of capillaries (Fig. 2*C*, arrows) within the endomysium (i.e., the extracellular connective tissue surrounding the muscle cells) (Fig. 2*B*). By 9 months, there appears to be progression of amyloid from the capillaries to the surrounding endomysial connective tissue (Fig. 2*D*, arrows), although the mechanism is unclear. Extensive amyloidosis within the endomysium was observed by 18 months of age (Fig. 2*E*) with occasional punctate deposits within some muscle fibers (Fig. 2*E*, arrow). Amyloid was present in heart and striated muscle but was not observed in any other tissue from D187N mice. Gelsolin amyloid was not observed at any age in WT muscle tissue (Fig. 2*F*). A temporal comparison of the D187N (+/+) and (−/+) muscle cross-sections from 1 to 18 months using CR fluorescence revealed more severe amyloidosis in the D187N (+/+) mice (Fig. S3), with much earlier deposition in the D187N (+/+) mice (≈1 month versus ≈3 months) (Fig. S3), consistent with the ≈2-fold increase in expression (Fig. 1 *C* and *D*).

Ultrastructural analysis of D187N (−/+) muscle cross-

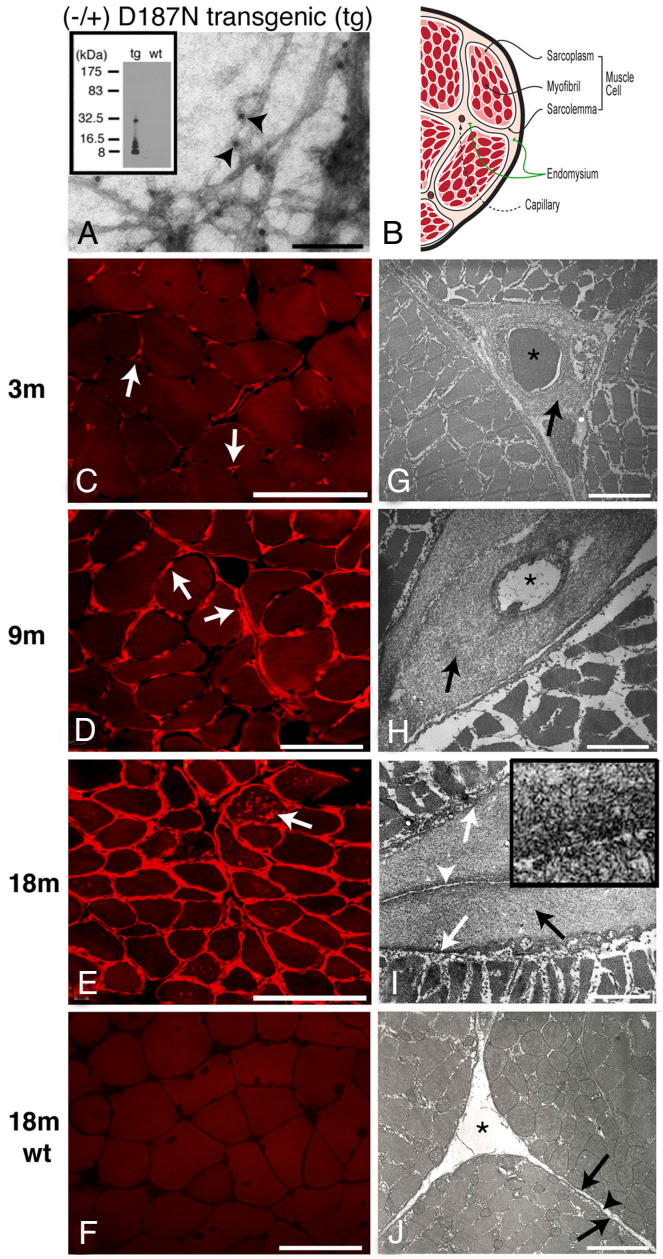

Fig. 2. Muscle of hemizygous D187N (−/+) gelsolin mice exhibit extensive amyloidogenesis. (*A*) EM analysis of amyloid extracted from 18-month D187N (−/+) muscle. Fibers, labeled with anti-FAF antibodies, were observed in (−/+) transgenic (tg) mice (*A*, arrowheads indicate the 10-nm gold particles) but not in wild-type siblings. The material obtained from D187N (−/+) muscle comprised primarily the 8-kDa fragment of human D187N plasma gelsolin (see *Inset*). (*B*) Schematic of a cross-section of a muscle fiber having the same orientation as *C–J*. (*C–J*) Cross-sections of muscle fibers were analyzed in D187N (−/+) mice at 3 months (*C* and *G*), 9 months (*D* and *H*), and 18 months (*E* and *I*), and in 18-month wild-type controls (*F* and *J*). In 3-month mice, CR deposits were localized exclusively around endomysial capillaries (*C*, arrows). By 9 months, CR reactivity was present around endomysial capillaries but also extended into the endomysium (*D*, arrows). At 18 months, CR reactivity surrounded all myofibers with several fibers also showing internal sarcoplasmic deposits (*E*, arrow). No CR positivity (*F*) was seen in 18-month wild-type mice. Electron micrographs confirmed fibrillar deposits in a pericapillary localization in 3-month D187N (−/+) mice (*G*, arrow). At 9 months, more extensive fibrillar deposits surrounded capillaries (*H*, arrows) and also extended into the endomysium. Thick pericapillary and endomysial fibrillar deposits (*I*, black arrow) were found in 18-month D187N (−/+) muscle. The large fibrillar deposits were between the sarcolemma (*I*, white arrows) of adjacent cells and the connective tissue of the endomysium (*I*, white arrowhead) and were absent in wild-type siblings [*J*, sarcolemma (arrows); endomysium (arrowhead)]. Capillaries are indicated with an asterisk (*). The high-magnification *Inset* (*I*) shows the fibrillar nature of the deposits. (Scale bars: *A*, 100 nm; *C–F*, 100 μm; *G*, 3.3 μm; *H*, 2.2 μm; *I*, 2.0 μm; *I Inset*, 0.3 μm; *J*, 2.0 μm.)

sections by EM confirmed the amyloid detected by CR fluorescence. Fibrillar deposits were first observed surrounding the capillaries at 3 months of age [Fig. 2*G*, arrow; capillaries are designated by an asterisk (*)]. Immuno-EM detection of deposition in younger mice may be possible by using antibodies specific for the 8-kDa fragment. Extensive amyloid deposition surrounding the capillaries was observed by 9 months of age (Fig. 2*H*, arrow). Older D187N (−/+) mice (9–18 months) also exhibited substantial fibrillar deposits between the sarcolemma (the limiting membrane of the muscle cell associated with its glycan coat) and the endomysium [Fig. 2*I*, black arrow indicates fibrillar deposits; white arrowhead indicates the endomysium that is no longer in contact with the sarcolemma (denoted by white arrows)]. No fibrillar deposits were found in wild-type mouse muscle (Fig. 2*J*, arrowhead denotes endomysium; arrows indicate sarcolemma). The progressive accumulation of amyloid in the endomysium may restrict normal metabolite exchange with the capillary, contributing to disease.

Amyloid Pathology in D187N Mice Progresses to a Histological Phenotype Resembling sIBM. Frozen muscle sections collected at 3, 9, and 18 months of age from D187N (−/+) mice (Fig. 3 *A–C*) and wild-type mice (Fig. 3 *D–F*) were evaluated using H&E staining. Three-month-old D187N (−/+) muscle was histologically similar to wild-type controls [Fig. 3, compare *A* (tg) and *D* (wt)], but by 9 months there was variability in myofiber size in D187N (−/+) mice with scattered muscle fibers exhibiting a granular blue basophilic appearance (Fig. 3*B*, arrows), consistent with degeneration and accumulation of intracellular protein aggregates. By 18 months, variability in D187N (−/+) myofiber size was more extensive, and numerous fibers had a basophilic appearance (Fig. 3*C*, arrows). Several fibers contained vacuoles (Fig. 3*C*, arrowheads) and inclusions (Fig. 3*C Inset*, arrows). The only abnormality identified in 18-month-old wild-type muscle was small, blue-rimmed vacuoles (Fig. 3*F*, arrowheads) typical of an aged rodent. The WT vacuoles and their contents were CR fluorescence negative.

In older homozygous D187N (+/+) mice (12–18 months), there was extensive myofiber atrophy with increased numbers of fibers exhibiting vacuoles (Fig. 3*G*, black arrows) and inclusions (Fig. 3*H*, arrowhead) and lipid accumulation (Fig. 3*G*, arrowheads). Moreover, CR fluorescence observed within the endomysium and in deposits within the muscle fibers of 18-month-old D187N (+/+) mice (Fig. S3 and Fig. 3 *H* and *I*, arrowheads) suggests the presence of amyloid. D187N (+/+) muscle had more prevalent multifocal areas of mononuclear cell infiltrations with a perivascular and endomysial distribution (Fig. 3 *G* and *H*, white arrows) relative to D187N (−/+) muscle. EM analysis revealed distended mitochondria, some of which contained inclusions (Fig. 3*J*, arrow), vacuoles containing tubulomembranous structures and myeloid bodies (Fig. 3 *K* and *L*, arrowheads), as well as filamentous inclusions within the sarcoplasm (Figs. 2*B* and 3*L*, arrow). The changes identified in both the hemizygous D187N (−/+) muscle and, more dramatically, in the homozygous D187N (+/+) muscle are reminiscent of the most common human muscle disease, sIBM (19–21, 27).

sIBM-Associated Aggregated Proteins Are Present Within the Muscle Fibers and Vacuoles of D187N Mice. Given the CR-positive fluorescence of the intracellular muscle inclusions, we examined whether these inclusions contained gelsolin. By using an anti-8-kDa gelsolin antibody, we detected gelsolin not only in the

CELL BIOLOGY

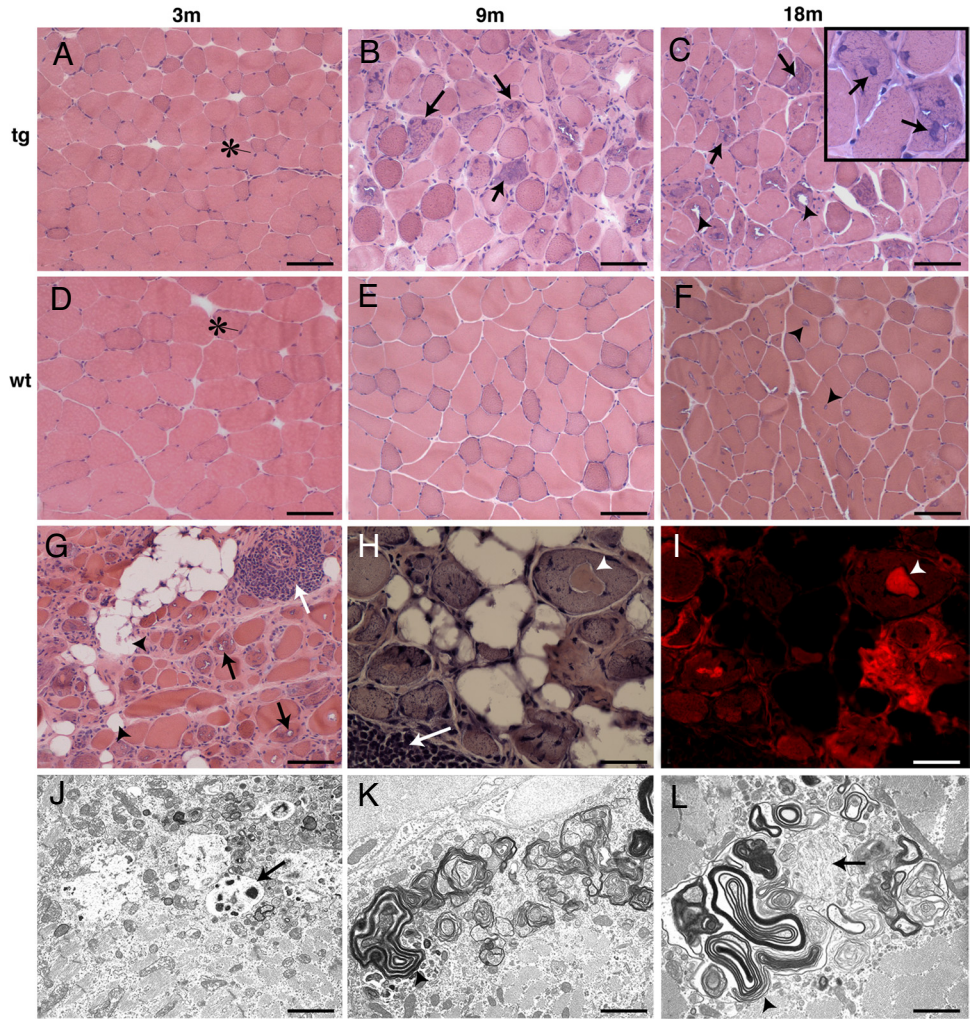

Fig. 3. D187N gelsolin mice exhibit age-related increases in muscle fiber atrophy and display morphological and histochemical characteristics of human sIBM. (*A–F*) H&E staining of cross-sections of muscle fibers in 3-, 9-, and 18-month-old mice. There were no pathological changes in 3-month D187N (−/+) mice (*A*). By 9 months, there was excessive variability in myofiber size with atrophic fibers having a basophilic appearance (*B*, arrows). At 18 months, atrophic fibers and fibers containing internal nuclei, basophilic inclusions (*C*, arrows; *Inset*, arrows), and vacuoles (*C*, arrowheads) were prominent. With the exception of small sarcoplasmic vacuoles that are common in aged rodents (*F*, arrowheads), no histological abnormalities were found in wild-type (wt) animals [3 months (*D*), 9 months (*E*), and 18 months (*F*)]. The asterisk (*) indicates the normal myofiber nuclei that are found toward the periphery of the cell. (*G–L*) H&E stain in homozygous D187N (+/+) mice revealed severe myopathic changes at an earlier age (*G*, 12 months; *H*, 18 months) including numerous atrophic fibers, endomysial amyloidogenesis, vacuoles (*G*, black arrows) and fatty infiltration (*G*, arrowheads), basophilic sarcoplasmic inclusions (*H*, arrowhead), and foci of mononuclear cell infiltration (*G* and *H*, white arrows). CR positivity was extensive (*I*), including endomysial and sarcoplasmic deposits (*I*, arrowhead) (*H* and *I*, same cells are shown). Electron microscopy showed distended mitochondria, some with inclusions (*J*, arrow), vacuoles containing tubulomembranous structures and myeloid bodies (*K* and *L*, arrowheads), and sarcoplasmic fibrillar deposits (*L*, arrow). (Scale bars: *A–G*, 100 μm; *H* and *I*, 25 μm; *J*, 2.9 μm; *K*, 1.7 μm; *L*, 1.4 μm.)

endomysium (Fig. 4*A*, arrowhead) but also in the intracellular deposits (Fig. 4*A*, arrow). Intracellular deposits found in sIBM typically contain multiple proteins associated with extracellular human amyloid diseases including the amyloid precursor protein (APP) and its amyloidogenic fragment Aβ, as well as an overrepresentation of ubiquitinated proteins. Immunofluorescence using an Aβ-specific antibody revealed intracellular Aβ peptide accumulation (Fig. 4*B*, arrowhead), as shown in a serial section of a cell where the sarcolemma is identified by staining with anti-sarcoglycan (Figs. 2*B* and 4*C*, arrow). Intracellular accumulation of APP (Fig. 4*D*, arrows) and ubiquitinated proteins (Fig. 4*E*, arrows) was also observed in homozygous D187N (+/+) muscle. Consistent with these results, the expression level of APP in D187N gelsolin (+/+) muscle is substantially increased compared with wild-type muscle (Fig. 4*F*), analogous to what is seen in human sIBM (21, 28). In addition, the Aβ peptide resulting from proteolysis of APP can be detected in D187N gelsolin (+/+) muscle, but not in wild-type muscle, indicating accumulation of Aβ in D187N (+/+) muscle fibers (Fig. 4*G*, arrow indicates monomer), as occurs in human sIBM. The higher molecular mass bands in Fig. 4*G* are likely Aβ oligomers within D187N (+/+) muscle.

Homozygous D187N (+/+) Mice Display Significant Muscle Weakness. Although the integrity of the muscle structure in both hemizygous D187N (−/+) and homozygous D187N (+/+) mice was compromised, only the homozygous D187N (+/+) mice show signs of muscle weakness at 12–14 months of age according to grip strength analysis (Fig. S4). Loss of muscle strength was progressive in homozygous mice, with the first indication of the defect at 7–9 months of age (Fig. S4). Alternative muscle strength assessments, such as the challenging beam traversal, revealed analogous results (Fig. S5). It may be that analysis of much older (−/+) mice will reveal a muscle weakness pheno-

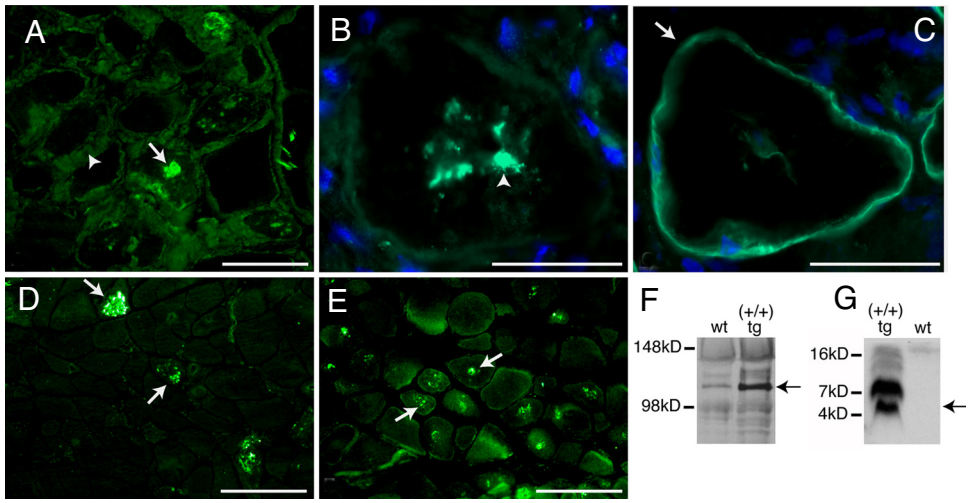

Fig. 4. Amyloid and sIBM associated proteins are detected within the muscle fibers of D187N (+/+) mice. (*A–E*) Immunohistochemistry of cross-sections of frozen D187N (+/+) muscle. D187N gelsolin localized to both the endomysium (*A*, arrowhead) and in the intracellular inclusions (*A*, arrow). Serial sections revealed intracellular accumulation of Aβ1–42 (*B*, arrowhead) within a cell with the sarcolemma identified with anti-α-sarcoglycan (*C*, arrow). Anti-APP (*D*, arrow) and anti-ubiquitin (*E*, arrow) also label the intracellular inclusions. (*F*) Immunoblots of D187N (+/+) transgenic (tg) and wild-type (wt) muscle homogenates with anti-APP indicate higher levels of full-length APP in tg muscle (arrow). (*G*) Blots probed with anti-Aβ showed Aβ peptide monomer (arrow) and oligomeric species present in D187N (+/+) tg but not wt muscle extracts. (Scale bars: *B* and *C*, 50 μm; *A*, *D*, and *E*, 100 μm.)

type. The muscular weakness observed in the homozygous D187N (+/+) gelsolin mice is consistent with the clinical findings in both sIBM and FAF patients (18, 19).

Discussion

The D187N gelsolin amyloidosis mouse models accurately recapitulate the proteolytic cascade that yields the 8- and 5-kDa amyloidogenic peptides that putatively cause FAF. Notably, the amyloidogenesis is restricted to the muscle tissues where D187N gelsolin is synthesized. That this occurs, despite the presence of high levels of full-length and C68 D187N gelsolin in the plasma, strongly suggests that amyloid deposition in human FAF arises from local synthesis, furin proteolysis during secretion, proximal extracellular MT1-MMP proteolysis, and deposition in the local extracellular matrix, and not from transcytosis of plasma gelsolin across vessel walls. Whether deposition progresses from a single focal origin to proximal cells or through random autonomous initiation is unknown. Mice expressing D187N gelsolin under the ubiquitin C promoter exhibit amyloid in multiple tissues and the load correlates with local D187N gelsolin expression levels, supporting the local deposition hypothesis. This hypothesis is also consistent with the avascular human cornea being one of the first organs to exhibit gelsolin amyloidogenicity.

In addition, the D187N (+/−) and D187N (+/+) human gelsolin mouse lines exhibit an aging-associated decline in cellular proteostasis (1, 9), reflected by amyloid-like intracellular inclusions containing the Aβ peptide, APP, and other amyloidogenic polypeptides, as well as ubiquitinated proteins: a characteristic resembling human sIBM, the most common aging-associated muscle disease (19). Human sIBM muscle biopsies suggest that proinflammatory mediators such as IL-1β induce overexpression of APP leading to intracellular Aβ deposition (demonstrated in human myotubes) that in turn may induce further inflammation (21, 29). Other characteristics of sIBM include mononuclear cell infiltration, blue-rimmed vacuoles, mitochondrial defects, and progressive muscle weakness (19).

One hypothesis for how sIBM may be triggered in the FAF mouse model is that the increased demand placed on the proteostasis network by the presence of the misfolding-prone D187N gelsolin protein in the secretory pathway and/or the extracellular aggregation of its fragments during aging exceeds the ability of the mouse muscle tissue to maintain proteostasis (1, 3). In support of this, introduction of a cytosolic temperature-sensitive, misfolding-prone protein into a huntingtin's *Caenorhabditis elegans* model exacerbates the huntingtin proteotoxicity phenotype at the restrictive temperature on aging (5). Although the etiology of sIBM remains to be determined, the observations that the secretion of amyloidogenic gelsolin or transthyretin mutants (30), or increased secretion of APP (and Aβ) increase the risk for developing sIBM (31), are consistent with the hypothesis that consumption of proteostasis capacity (e.g., chaperone, disaggregase, and degradation activities) by misfolded and/or aggregation-prone proteins (1, 9) could be responsible for triggering human sIBM upon aging, perhaps in part by inflammatory pathway signaling known to result in APP overexpression (21, 29, 32). Although WT plasma gelsolin overexpression in mice and in cell lines does not lead to aberrant proteolysis or gelsolin amyloidosis (24, 33), it remains a possibility that WT gelsolin overexpression in muscle cells could trigger sIBM. We think this is unlikely because WT plasma gelsolin has been expressed in Alzheimer's transgenic mice (albeit in hepatocytes, thus not comparable with the muscle-mediated expression used in our studies) and administered to rodent disease models (33, 34), and in all cases, WT gelsolin protected the animals from the pathology being studied.

In summary, we have created transgenic FAF mouse models. It appears that local D187N synthesis, aberrant proteolysis, and localized deposition result in FAF. The ability to detect C68 and the 8-kDa amyloidogenic fragment, as well as amyloid in (+/+) mice as young as 1 month of age, along with the muscle weakness phenotype at 7–9 months of age, now allows us to evaluate therapeutic strategies for FAF, and potentially sIBM. These include inhibition of furin, inhibition of MT1-MMP (12), antagonism of the glycosaminoglycan gelsolin fragment interactions (23), and use of proteostasis regulators (1, 7) that enhance proteostasis capacity.

Materials and Methods

Immunoblots. Antibodies used were an anti-FAF antibody (directed against the human 8-kDa amyloidogenic peptide) that does not recognize mouse gelsolin (12), anti-APP (CT695; Invitrogen), or anti-Aβ (4G8; Sigma). See *SI Methods* for description of sample preparation.

Light and Electron Microscopy. Unfixed cryosections (8 μm) of muscle were stained with H&E or for CR fluorescence localization. For ultrastructural

analysis by electron microscopy, thin sections (60–90 nm) of glutaraldehyde-fixed muscle specimens were stained with uranyl acetate and lead citrate before examination in an electron microscope. A detailed method is provided in *SI Methods*.

Immunofluorescence. Unfixed cryosections (8 μm) were stained with antibodies against anti-FAF (12), anti-APP (Invitrogen), anti-Aβ 1–42 (Abcam), anti-ubiquitin (Dako), and anti-α-sarcoglycan (a gift from E. Engvall, The Burnham Institute for Medical Research, La Jolla, CA).

Amyloid Isolation and Analysis. Using a Teflon mechanical homogenizer (80 rpm) at 4 °C, muscle tissues were minced and homogenized in 150 mM NaCl until no solid tissue was visible. Amyloid isolated from the tissues was analyzed by immuno-EM by using anti-FAF antibodies and protein A-gold (10 nm).

Grip Strength. The muscle function of the animals was assessed by using a grip strength meter (for details of the method, see *SI Methods*). The force at which the animal released its grip was measured for 5 trials and then averaged. Group means were analyzed with ANOVA followed by Fisher's least significant difference.

ACKNOWLEDGMENTS. We thank S. Hauschka (University of Washington, Seattle, WA) for kindly providing the muscle creatine kinase promoter, Marie-Françoise Chesselet and J. Conkright for help and advice in generating and analyzing the mice, and Colleen Fearns and James Solomon for assistance with manuscript preparation. This work was supported by National Institutes of Health Grants AG18917 (to J.W.K.), GM33301 (to W.E.B.), and P50NS38367 (to M.-F. Chesselet, The David Geffen School of Medicine), and the American Parkinson Disease Association (S.M.F.).

1. Balch WE, Morimoto RI, Dillin A, Kelly JW (2008) Adapting proteostasis for disease intervention. *Science* 319:916–919.
2. Morley JF, Brignull HR, Weyers JJ, Morimoto RI (2002) The threshold for polyglutamine-expansion protein aggregation and cellular toxicity is dynamic and influenced by aging in *Caenorhabditis elegans*. *Proc Natl Acad Sci USA* 99:10417–10422.
3. Cohen E, Bieschke J, Perciavalle RM, Kelly JW, Dillin A (2006) Opposing activities protect against age-onset proteotoxicity. *Science* 313:1604–1610.
4. Erickson RR, Dunning LM, Holtzman JL (2006) The effect of aging on the chaperone concentrations in the hepatic, endoplasmic reticulum of male rats: The possible role of protein misfolding due to the loss of chaperones in the decline in physiological function seen with age. *J Gerontol A Biol Sci Med Sci* 61:435–443.
5. Gidalevitz T, Ben-Zvi A, Ho KH, Brignull HR, Morimoto RI (2006) Progressive disruption of cellular protein folding in models of polyglutamine diseases. *Science* 311:1471–1474.
6. Wang X, et al. (2006) Hsp90 cochaperone Aha1 downregulation rescues misfolding of CFTR in cystic fibrosis. *Cell* 127:803–815.
7. Mu TW, et al. (2008) Chemical and biological approaches synergize to ameliorate protein-folding diseases. *Cell* 134:769–781.
8. Gitler AD, et al. (2008) The Parkinson's disease protein alpha-synuclein disrupts cellular Rab homeostasis. *Proc Natl Acad Sci USA* 105:145–150.
9. Powers ET, Morimoto RI, Dillin A, Kelly JW, Balch WE (2009) Biological and chemical approaches to diseases of proteostasis deficiency. *Annu Rev Biochem* 78:959–991.
10. Tanzi RE, Bertram L (2005) Twenty years of the Alzheimer's disease amyloid hypothesis: A genetic perspective. *Cell* 120:545–555.
11. Chen CD, et al. (2001) Furin initiates gelsolin familial amyloidosis in the Golgi through a defect in Ca^{2+} stabilization. *EMBO J* 20:6277–6287.
12. Page LJ, et al. (2005) Metalloendoprotease cleavage triggers gelsolin amyloidogenesis. *EMBO J* 24:4124–4132.
13. Huff ME, Page LJ, Balch WE, Kelly JW (2003) Gelsolin domain 2 Ca^{2+} affinity determines susceptibility to furin proteolysis and familial amyloidosis of Finnish type. *J Mol Biol* 334:119–127.
14. Kiuru S (1998) Gelsolin-related familial amyloidosis, Finnish type (FAF), and its variants found worldwide. *Amyloid* 5:55–66.
15. Smith DB, Janmey PA, Herbert TJ, Lind SE (1987) Quantitative measurement of plasma gelsolin and its incorporation into fibrin clots. *J Lab Clin Med* 110:189–195.
16. Kwiatkowski DJ, Mehl R, Izumo S, Nadal-Ginard B, Yin HL (1988) Muscle is the major source of plasma gelsolin. *J Biol Chem* 263:8239–8243.
17. Kangas H, Seidah NG, Paunio T (2002) Role of proprotein convertases in the pathogenic processing of the amyloidosis-associated form of secretory gelsolin. *Amyloid* 9:83–87.
18. Kiuru-Enari S, Somer H, Seppalainen AM, Notkola IL, Haltia M (2002) Neuromuscular pathology in hereditary gelsolin amyloidosis. *J Neuropathol Exp Neurol* 61:565–571.
19. Engel WK, Askanas V (2006) Inclusion-body myositis: Clinical, diagnostic, and pathologic aspects. *Neurology* 66:S20–S29.
20. Sugarman MC, et al. (2006) Pathogenic accumulation of APP in fast twitch muscle of IBM patients and a transgenic model. *Neurobiol Aging* 27:423–432.
21. Schmidt J, et al. (2008) Interrelation of inflammation and APP in sIBM: IL-1 beta induces accumulation of beta-amyloid in skeletal muscle. *Brain* 131:1228–1240.
22. Maury CP (1991) Gelsolin-related amyloidosis. Identification of the amyloid protein in Finnish hereditary amyloidosis as a fragment of variant gelsolin. *J Clin Invest* 87:1195–1199.
23. Suk JY, Zhang F, Balch WE, Linhardt RJ, Kelly JW (2006) Heparin accelerates gelsolin amyloidogenesis. *Biochemistry* 45:2234–2242.
24. Paunio T, et al. (1994) Toward understanding the pathogenic mechanisms in gelsolin-related amyloidosis: In vitro expression reveals an abnormal gelsolin fragment. *Hum Mol Genet* 3:2223–2229.
25. Linke RP (2000) Highly sensitive diagnosis of amyloid and various amyloid syndromes using Congo red fluorescence. *Virchows Arch* 436:439–448.
26. Howie AJ, Brewer DB, Howell D, Jones AP (2008) Physical basis of colors seen in Congo red-stained amyloid in polarized light. *Lab Invest* 88:232–242.
27. Paciello O, Wojcik S, Engel WK, McFerrin J, Askanas V (2006) Parkin and its association with a-synuclein and AbetaPP in inclusion-body myositis and AbetaPP-overexpressing cultured human muscle fibers. *Acta Myol* 25:13–22.
28. Sarkozi E, Askanas V, Johnson SA, Engel WK, Alvarez RB (1993) beta-Amyloid precursor protein mRNA is increased in inclusion-body myositis muscle. *Neuroreport* 4:815–818.
29. Zhang K, Kaufman RJ (2008) From endoplasmic-reticulum stress to the inflammatory response. *Nature* 454:455–462.
30. Askanas V, Engel WK, McFerrin J, Vattemi G (2003) Transthyretin Val122Ile, accumulated Abeta, and inclusion-body myositis aspects in cultured muscle. *Neurology* 61:257–260.
31. Sugarman MC, et al. (2002) Inclusion body myositis-like phenotype induced by transgenic overexpression of beta APP in skeletal muscle. *Proc Natl Acad Sci USA* 99:6334–6339.
32. Lee RK, Wurtman RJ (2000) Regulation of APP synthesis and secretion by neuroimmunophilin ligands and cyclooxygenase inhibitors. *Ann NY Acad Sci* 920:261–268.
33. Hirko AC, Meyer EM, King MA, Hughes JA (2007) Peripheral transgene expression of plasma gelsolin reduces amyloid in transgenic mouse models of Alzheimer's disease. *Mol Ther* 15:1623–1629.
34. Rothenbach PA, et al. (2004) Recombinant plasma gelsolin infusion attenuates burn-induced pulmonary microvascular dysfunction. *J Appl Physiol* 96:25–31.